LUNAR INTRUSIVE DOMES ON THE FLOOR OF GRIMALDI AND NEAR ARISTILLUS. C. Wöhler[1,2], R. Lena[3], K. C. Pau[4] – Geologic Lunar Research (GLR) Group. [1]Daimler Group Research and Advanced Engineering, D-89013 Ulm, Germany; christian.woehler@daimler.com; [2]Applied Informatics, Faculty of Technology, Bielefeld University, D-33615 Bielefeld, Germany; [3]Via Cartesio 144, sc. D, I-00137 Rome, Italy; r.lena@sanita.it; [4]Flat 20A, Fook Chak House, Tung Fai Gardens, 17 Po Yan Street, Sheung Wan, Hong Kong; kcpaulhk@yahoo.com.hk

Introduction: Lunar domes may form as effusive shield-like volcanoes, or the magma may remain subsurface as a laccolith, resulting in an up-doming of the surface. Under the assumption of an intrusive origin of several domes previously examined in [1, 2], we utilise the laccolith model introduced in [3] to estimate the corresponding geophysical parameters, especially the intrusion depth and magma pressure [2]. The four domes Ga1, V1, M13 and Ar1, belonging to class In1 of probably intrusive domes introduced in [2], are all of elongated shape and associated with faults or linear rilles on their surfaces. The pronounced tensional features suggest a formation of these domes by laccolithic intrusions, leading to flexuring and up-doming of the mare surface. An analogous suggestion is given in [4] to explain the occurrence of tensional linear rilles on some lunar kipukas. Intrusive dome class In1 comprises large features with diameters exceeding 25 km and flank slopes between 0.2° and 0.6°. Class In2 is made up by smaller and slightly steeper domes with diameters between 10 and 15 km and flank slopes higher than 0.4°, reaching maximum values of about 0.8°. Domes of class In3 have moderate diameters between 13 and 20 km and very low flank slopes of less than 0.3°. In this contribution we provide an analysis of two further candidate intrusive domes. The first dome, termed Grimaldi 1 (Gr1), is located on the floor of the Grimaldi basin at 68.62° W and 4.45° S and has an elongated base area of 36 x 24 km² (cf. Fig. 1). Several straight rilles can be distinguished on its surface, which are likely due to tensional stress consistent with laccolith formation. The second examined dome, termed Aristillus 1 (Ari1), is located near the crater Aristillus at 5.67° E and 33.28° N and has an elongated base area of 54 x 35 km². This dome is clearly apparent in the low-sun telescopic CCD images shown in Fig. 2 but is hardly visible under moderate solar illumination angles (cf. Fig. 3).

Geologic setting: Grimaldi is a small impact basin of Pre-Nectarian age. Its main ring has a diameter of 440 km and an average depth of 3.2 km, while the inner ring has a diameter of about 140 km [5]. The inner wall of Grimaldi has been eroded by subsequent impacts such that it forms a low, irregular ring of hills, ridges, and peaks rather than a typical crater rim. Orbiting spacecraft have also detected a mascon below Grimaldi [6, 7]. The large and flat dome Gr1 is located on the relatively smooth basin floor. Its overall shape is similar to that of the well-known Valentine dome, termed V1 in [2]. Several non-volcanic hills protrude through the dome surface, and a small flat-floored depression occurs just off-center (cf. Fig. 1). The second examined dome, Ari1, is located close to the crater Aristillus in eastern Mare Imbrium (cf. Fig. 2). Both domes are not visible in Lunar Orbiter imagery (cf. Fig. 4) acquired under moderate solar elevation angles. However, it is clearly apparent in Fig. 4 that both domes are characterised by several straight rilles traversing their surfaces and by small non-volcanic hills.

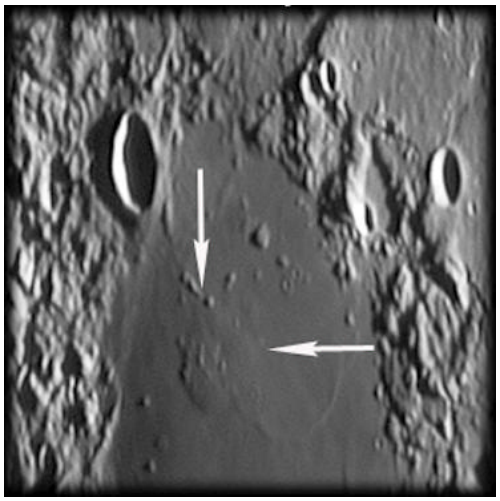

Fig. 1: Dome Gr1 on the floor of Grimaldi. Telescopic CCD image acquired on November 11, 2008, at 13:23 UT.

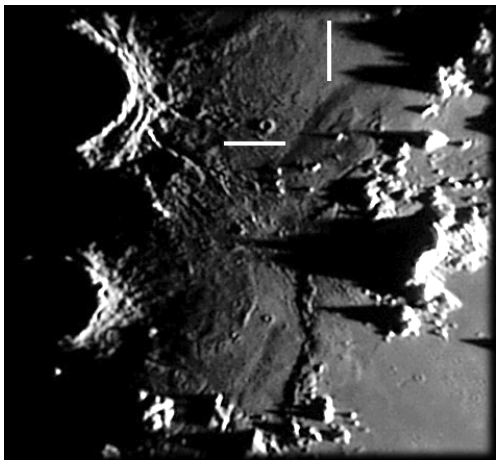

Fig. 2: Dome Ari1 near the crater Aristillus. Telescopic CCD image acquired on May 01, 2009, at 19:30 UT.

Spectral properties: Clementine UVVIS data reveal that the surface of Gr1 has a fairly high 750 nm re-

flectance of 0.1129 and a R_{415}/R_{750} ratio of 0.5948, indicating a moderate TiO_2 content. The R_{950}/R_{750} ratio of 1.0680 implies a weak mafic absorption, suggesting a high soil maturity. The dome Ari1 has a similarly high 750 nm reflectance of 0.1023. It is spectrally red with a low R_{415}/R_{750} ratio of 0.5864, indicating a lower TiO_2 content than Gr1, while its high R_{950}/R_{750} ratio of 1.0447 suggests a high soil maturity of the dome surface. Both domes do not display a spectral contrast with respect to the mare surface surrounding them.

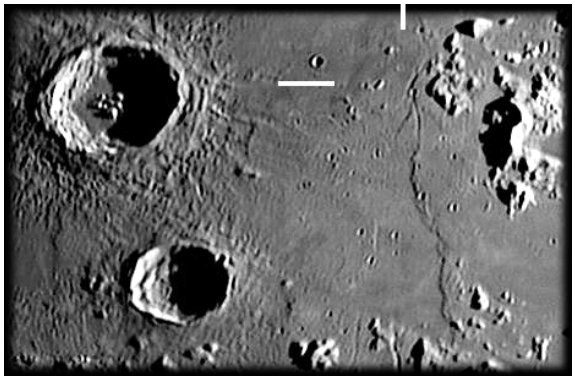

Fig. 3: Dome Ari1 near the crater Aristillus. Telescopic CCD image acquired on October 26, 2009, at 18:05 UT.

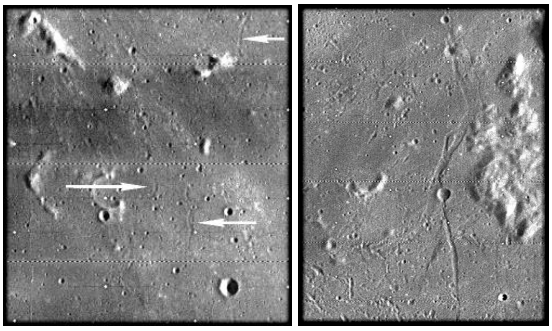

Fig. 4: Left: Lunar Orbiter image IV-168-H3. Arrows indicate short rilles on the surface of Gr1. Right: Lunar Orbiter image IV-110-H1, showing straight rilles on the surface of Ari1.

Morphometric dome properties: Based on the telescopic CCD images shown in Figs. 1 and 2, which were acquired under oblique solar illumination, we determined DEMs of the examined domes by applying the combined photoclinometry and shape from shading method described in [8]. The heights and flank slopes of the domes were extracted from the DEMs (Table 1). The heights of Gr1 and Ari1 correspond to 160 m and 85 m, respectively, resulting in average flank slopes of 0.62° and 0.22°. The dome volume was extracted from the DEM for Gr1 and estimated by assuming a parabolic dome shape for Ari1, resulting in edifice volumes of 75 km³ and 63 km³, respectively. It has been shown in [8] that the relative error of the height and slope values amounts to 10% while the relative accuracy of the dome volume is about 20%. We also estimated the height of the dome Gr1 based on shadow length measurements in the oblique illumination view shown in Fig. 1, where a value of 145 ± 15 m was obtained.

Laccolith modelling: If we assume that the linear rilles on the surfaces of Gr1 and Ari1 are the result of tensional stress, the curvature radii of the dome surfaces inferred from our 3D analysis yield thicknesses of the uppermost mare basalt layer of at least 0.7 and 1.1 km, respectively, assuming a typical value of the critical stress of basalt of 13 MPa [9]. The laccolith model in [3] applied according to the numerical scheme suggested in [2] yields intrusion depths of 2.4 km and 7.9 km and maximum magma pressures in the laccolith of 19 MPa and 66 MPa, respectively (cf. Table 1). The inferred intrusion depth and magma pressure of Gr1 is comparable to values obtained for other probably intrusive domes of class In1 [2], such as the Valentine dome V1 and the dome Ga1 near the crater Gambart. The intrusion depth and magma pressure obtained for Ari1 are about twice as large as the corresponding values inferred for other domes of class In1 in [2]. According to the laccolith model, these high values are mainly a result of the exceptionally large size of Ari1.

dome	*slope [°]*	*size [km]*	*h [m]*	*V [km³]*	*h_1 [km]*	*d [km]*	*p_0 [MPa]*
Gr1	0.62	36x24	160	75	0.7	2.4	19
Ari1	0.22	54x35	85	63	1.1	7.9	66

Table 1: Morphometric properties of Gr1 and Ari1 and modelling results for the basaltic layer thickness h_1, intrusion depth d, and maximum magma pressure p_0.

Conclusion: The two low and large lunar domes Gr1 and Ari1 are interpreted as being formed by magmatic intrusion. It is unlikely that they are kipukas as no spectral contrast is apparent between them and the surrounding surface. Similar to previously examined lunar domes of presumably intrusive origin [2], Gr1 and Ari1 are of strongly elongated shape. Both domes display straight rilles traversing their surfaces, which are likely of tensional origin. Regarding the morphometric properties and modelling results, Gr1 is a typical representative of class In1, while the intrusion depth and magma pressure inferred for Ari1 exceed the range of previously modelled values by factors of 2–3.

References: [1] Lena and Wöhler (2008), *LPSC XXXIX*; [2] Wöhler and Lena (2009), *Icarus 204*; [3] Kerr and Pollard (1998), *J. Struct. Geol. 20(12)*; [4] Nichols et al. (1974), *LPSC V*; [5] Wilhelms (1987), *USGS Prof. Paper 1348*; [6] Kiefer (1999), *LPSC XXX*; [7] Kiefer (1997), *LPSC XXVIII*; [8] Wöhler et al. (2006), *Icarus 183*; [9] Pollard and Fletcher (2005), *Fundamentals of Structural Geology*, Cambridge University Press.